



Contents list available at IJRED website

International Journal of Renewable Energy Development

Journal homepage: <https://ijred.undip.ac.id>



Research Article

Design, optimization and economic viability of an industrial low temperature hot water production system in Algeria: A case study

Karim Kaci^{a*}, Mustapha Merzouk^a, Nachida Kasbadji Merzouk^b, Mohammed Missoum^c, Mohammed El Ganaoui^d, Omar Behar^e, Rabah Djedjig^d

^aLaboratoire de Physique Fondamentale et Appliquée Département des Energies Renouvelables, Faculté de Technologie, Université Blida, W. Blida, Algeria.

^bUnité de Développement des Equipements Solaires, UDES, Centre de Développement des Energies Renouvelables, CDER, 42004, W. Tipaza, Algérie.

^cDepartment of Mechanical Engineering, Faculty of Technology, University Center of Morceli, Abdellah, Tipaza, Algeria.

^dUniversity of Lorraine, LERMAB, IUT de Longwy, 186 rue de Lorraine, 54400 Cosnes-et-Romain, France.

^eCCRC, King Abdullah University of Science and Technology (KAUST), Thuwal, 23955, Saudi Arabia.

Abstract. Solar energy has a great potential in many areas of industrial activity in Algeria. This is because most of Algeria has high levels of sustainable solar insolation. Unfortunately, few industries use solar energy for hot water generation, but some industrial processes require hot water at temperatures that can be easily obtained from solar thermal panels. This paper presents a case study to investigate the technical and financial feasibility of a solar-powered industrial agro-processing system in Algiers. Based on the solar collectors connection type for which the economic feasibility study was carried out, an appropriate design of the system was determined. The latter was actually done by analyzing the levelized cost of energy savings. The design of the thermo-solar process is carried out based on F-chart method with a new approach by integrating the incidence angle modifier and of using real and experimental data requirements to determine realistic achievable performance of the solar process. The results showed that, in comparison to the currently used electrical system, the electrical energy savings achieved by the solar-powered system make it an economically viable option with a solar coverage rate of 80%. The investment depreciation balance shows that the use of such a thermal solar energy system will be more competitive than fossil fuels system if the price of electricity in the country increases from 0.048 to 0.075 €/kWh.

Keywords: Process industrial application, solar thermal collector, Thermo-solar system, Techno-economic assessment, water heating.



@ The author(s). Published by CBIORE. This is an open access article under the CC BY-SA license (<http://creativecommons.org/licenses/by-sa/4.0/>).

Received: 12th Nov 2022; Revised: 24th January 2023; Accepted: 6th March 2023; Available online: 21st March 2023

1. Introduction

In recent years, interest in solar development has increased in Algeria since the publication of the Renewable Energy and Energy Efficiency Plan 2016-2030 (The Minister of Energy Transition and Renewable Energies., 2022). The industrial sector is a promising area for the development of solar thermal technology, accounting for more than 25% of total final energy consumption (International Energy Agency, 2020). The efficiency of converting solar energy into heat (up to 70%) is much higher than converting it into electricity (about 15%), demonstrating the benefits of integrating solar thermal energy into industrial processes. The heating process consumes a lot of thermal energy. Globally, 50% of energy consumption is used for heating applications (Valderrama *et al.*, 2022). A great fraction (about 90%) of this heat comes from fossil fuels, which emit large amounts of greenhouse gas emissions and thus exacerbate the effects of climate change (Intergovernmental Panel on Climate Change IPCC (2022) Mitigation of Climate Change; Assessment Report on Climate Change). Statistics show that 60% of industrial processes use heat at temperatures below 400°C, while more than 30% operate at temperatures

below 100°C (Zühlsdorfa *et al.*, 2019). Therefore, integrating solar energy into industry can help to reduce the effects of climate change, especially in low-temperature processes. Nowadays, around 456 GWth of solar thermal output has been installed globally (National Renewable Energy Laboratory. 2021). Low temperature thermal industrial processes recorded growth of 1.5% in 2016 (Meyers *et al* 2018). According to a recent study, published by SOLIRCO, the industrial sector used 416 414 m² of installed space, 40% of which was used in the agro-food sector (The International Renewable Energy Agency. 2015)

In fact, the heat generated by solar thermal systems is less used in industry than in domestic applications (Renewable Energy Policy Network for the 21st Century. 2016). However, several studies related to the use of solar heat for industrial processes revealed that solar thermal industrial heating systems can achieve higher efficiencies compared to domestic applications, especially at lower temperatures (Farjana *et al.*, 2017 and Sharma., *et al* 2017). A study conducted by Schweiger *et al.* (2000) in the framework of the European project POSHIP, which focuses on evaluating the potential of industrial solar systems in Spain and Portugal, shows that the latter can supply

* Corresponding author
Email: kkaci2022@gmail.com (K. Kaci)

5804 GWh, or 3.6% of the total energy demand (Schweigeretal.,2000). Muller *et al.* (2004) investigated solar heating systems as part of the European project PROMISE, and found that Austria has an energy solar potential of 264 PJ, representing 30% of total energy consumption. About 32 % is used to generate thermal energy below 200 °C. Kalogirou *et al.* (2003) studied the potential of solar industrial process heating in Cyprus for different temperature levels. Similar studies have also been reported for Australia by Fuller *et al.*, (2011). Kummert *et al.* (2000) carried out an experimental study on installation of a thermo-solar process, considering typical daily profiles.

Several studies have proven that the application of solar thermal systems in industry can lead to significant energy savings. As a part of an IEA project SHC Task 33 Solar PECES task IV, several configurations for thermo-solar processes thermal systems have been carried out in several European countries (Weiss., 2005). Lima *et al.*, (2015) demonstrated the feasibility of integrating a thermal solar process in a hospital in Brazil. Surech el *et al.*, (2017) presented a techno-economic study on integrated thermal solar processes in the Indian textile industry. Anubhav *et al.*, (2016) developed a model of a thermal solar process for the automotive industry in 2016. The economic analysis shows a payback period of 18 months. Quijera *et al.*, (2011) studied the feasibility of integrating a solar thermal system into the dairy industry through mathematical modeling. Therefore, the work suggests that the solar thermal potential of the industrial processes studied is important and should be considered for future energy. Moreover, Akssas *et al.*, (2013) conducted a techno- economic analysis of a solar water heater for a hospital center in Batna in Algeria, to study the techno-economic feasibility of solar heating water integration. The results showed the possibility of significant energy savings with installation (Total annual provided energy = 1427,1MWh and a Total annual net reduction of GHG = 905,84 Tons of CO₂ (Pahlavana 2018).

Review of previously published studies and various applications demonstrate the great potential of integrating solar heat into industrial processes. To encourage the deployment of solar energy, real case studies must be investigated to provide accurate information about the performance and the costs of solar-powered industrial processes. In this direction, the objective of this work is to design, evaluate the energy performance and determine the costs of a thermo-solar process that would be integrated to a food industrial process in Algeria. The design of the thermo-solar process is carried out based on F-chart method with a new approach by integrating the incidence angle modifier and of using real and experimental data requirements to determine realistic achievable performance of the solar process. This methodology was implemented into Trnsys software to facilitate modeling and device management of the entire system. In the following, firstly the case study is presented, then the methodology used to design the different solar system components is detailed and finally the energy and economic performances of the whole thermo-solar system are evaluated.

2. Methodology

2.1. Presentation of the case study

The thermo-solar process system considered in this study is an agro-food industrial process producing flavors and perfumes located in Algiers, Algeria (Longitude: 2.95°E, latitude: 36.7°N and elevation: 350 m).

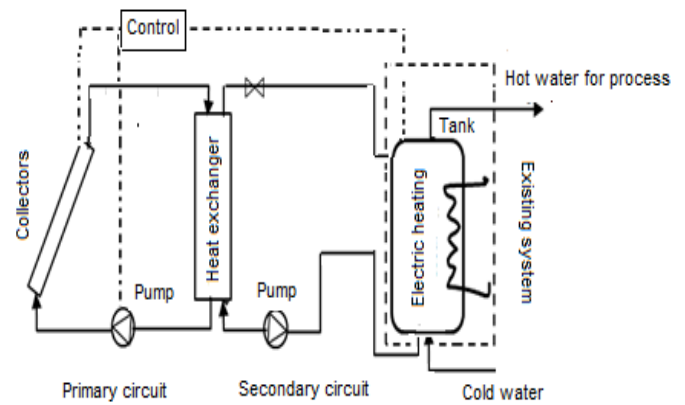


Fig. 1. Thermo-solar process into the industrial food process

The system consists of primary and secondary circuits as shown in Figure 1. The primary circuit includes a solar collector's field and a heat exchanger. Water is heated up in flat plate collectors and it is used as a working fluid to power a secondary circuit through water/water heat exchanger.

The secondary circuit feeds the industrial process and it is equipped with a storage tank which serves to store hot water to be used when solar energy is not enough available. Another heat exchanger is integrated in storage tank to provide high modularity to the system. A back-up electric heater is used in addition to the solar heating to ensure the continuous supply of hot water to the industrial process. For starting or stopping the pump, a regulation system was used. The thermo-solar process is designed to produce 3 m³/day of hot water at 60°C. The hourly daily load profile imposed by the used process is illustrated in Figure 2. The 3 m³ of hot water demand is situated between 11 to 12 am and 14 to 15 pm, which coincide with the availability of solar radiation.

2.2. Weather data and validation

Validation of the weather data model involves comparing predicted and measured solar radiation and ambient temperature. The measurements are provided by the Algiers Meteorological Station (Centre for the Development of Renewable Energy of Algeria., 2021), while the forecasts are obtained from the TRNSYS software (Meteonormsoftware8., 2022). Figure (3a) and (3b) highlight the measured solar radiation intensity and ambient temperature at the site of Algiers in 2020. A Good agreement between predicted and measured results was observed. The model demonstrated high accuracy in predicting the site's solar radiation and ambient temperature, allowing the system's performance to be estimated with reasonable accuracy.

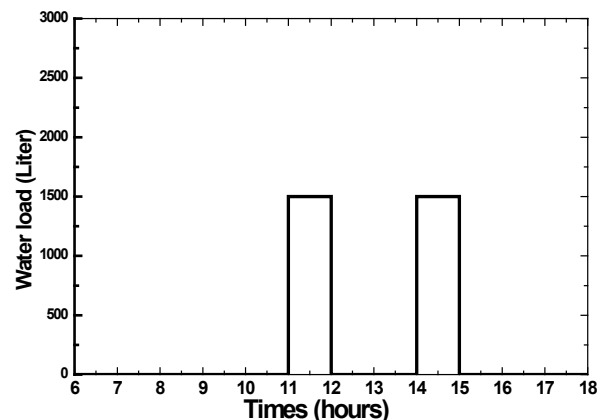


Fig. 2 Hourly daily load profile imposed by the process

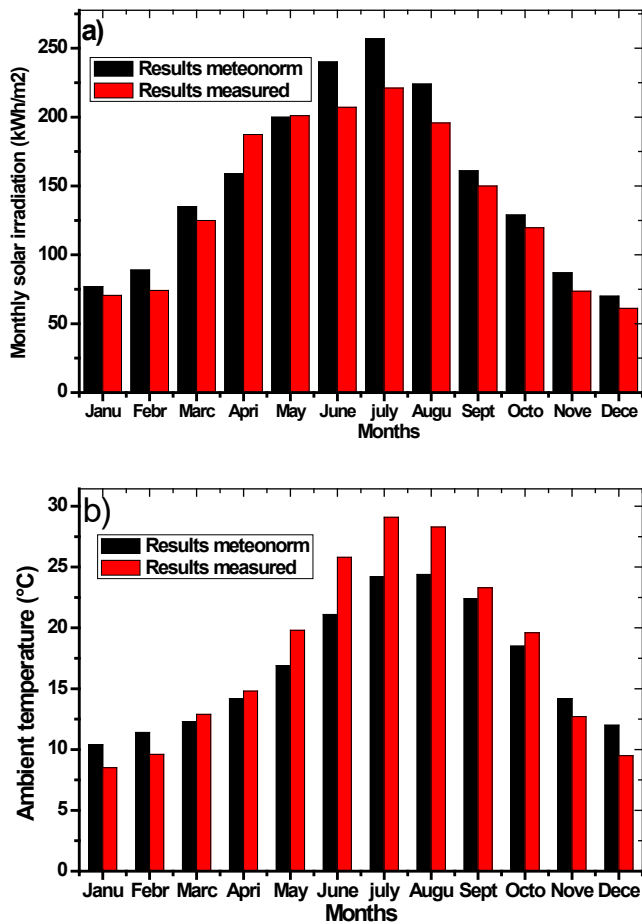


Fig.3 The radiometric parameters of the site a) Solar radiation data b) Ambient temperature

It can also be noted that the location has a high solar radiation intensity, reaching 250 kWh/m² in July, one of the highest potentials in the world, with an average ambient temperature of 18°C.

The temperature of cold water is an interesting parameter to determine the performance of the solar system. The monthly average ambient air and network water temperature provided by the software are shown in Figure 4 for a period of one year. The ambient temperature varies between 10 °C and 25 °C and average annual cold water temperature is about 18 °C. These values are the same of those provided by the Algerian Water Company (Ministry of Water Resources and Water Security, Algerian Waters, 2021). This means that the data provided by the software is accurate. The difference between summer and winter is significant. It can be seen that the temperature of cold water is 15°C in winter and reaches 25°C in summer, a difference of 10°C between these two periods, which affects strongly the system performance (Software Meteonorm 8. 2022).

Table 1
Conditions of parameters during testing

| Measurement parameters | Test conditions |
|--|------------------------------|
| Angle of incidence (θ) (°) | -55° to +55° |
| Total radiation on tilted surface I _g (W/m ²) | 840 < I _g < 950 |
| Diffuse radiation I _d (W/m ²) | 130 < I _d < 220 |
| Ambient temperature T _a (°C) | 20°C < T _a < 25°C |
| Mass flow rate, <i>m</i> (kg/s.m ²) | 0.02 +/- 10% |
| Wind velocity (V)-(m/s) | 1 < V < 3 |

Source: Kaci et al (2012)

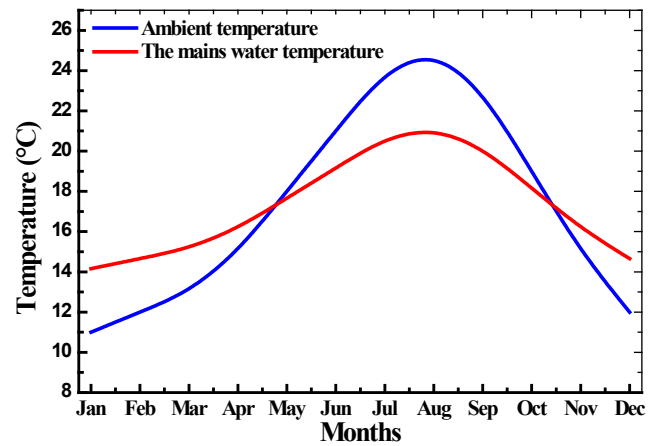


Fig.4 Variation of the mains water and ambient temperatures during a year

2.3. Determination of the solar collector's parameters

Before evaluating the energy performance of the solar water-heating system under investigation, an experimental study was carried out to determine the real characteristics of the solar collector used; namely the instantaneous efficiency and the modified incidence angle. According to the European standard, the fluctuations of the variables (incidence angle θ, ambient temperature T_a, global radiation I_g, mass flow rate *m* and wind speed V) are checked within the limit tolerated by the standard as given in Table 1.

The experimental study was carried out during different moments of four days, where inlet and outlet collector's temperatures, ambient temperature as well as the global radiation are measured. These parameters allow calculating the instantaneous efficiency of the solar collector η. Four inlet temperatures are considered (T_a, T_a+10, T_a+20, T_a+30). Each temperature is recorded for four times, two before noon and two in the afternoon, for a total of sixteen points. Table 2 shows the parameters measured during the test period.

The instantaneous efficiency may be given by the equation (1) (Kaci et al2012.)

$$\eta = \eta_0 - a_1 T^* \tag{1}$$

Where:

$$T^* = \frac{(T_e - T_a)}{I_g}$$

$\eta_0 = F_R(\tau\alpha)$ is the collector optical efficiency; and $a_1 = (F_R U_g)$ is the collector overall energy loss coefficient.

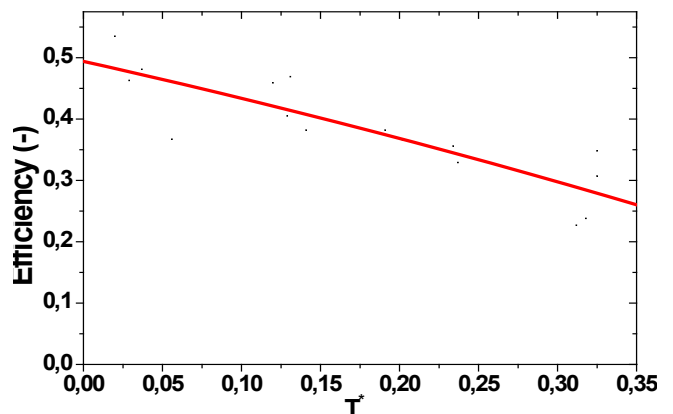


Fig. 5 Representation of the instantaneous performance of the collector

Table 2
Tests carried out to calculate the instantaneous yield

| Time (Hour) | Te (°C) | Ts (°C) | Ta (°C) | I _g (W/m ²) | T* (Km ² /W) | η |
|----------------|------------|------------|------------|---------------------------------------|----------------------------|------|
| 11:29 a.m | 21.45 | 25.04 | 18.61 | 815 | 0.056 | 0.36 |
| 11:44 a.m | 21.14 | 27.18 | 22.25 | 941 | 0.02 | 0.53 |
| 12:54 p.m | 20.46 | 25.72 | 20.28 | 950 | 0.029 | 0.46 |
| 01:09 pm | 20.82 | 26.31 | 20.01 | 954 | 0.037 | 0.48 |
| 11:09 a.m | 31.86 | 36.58 | 23.20 | 839 | 0.131 | 0.46 |
| 11:24 a.m | 31.72 | 36.39 | 23.79 | 850 | 0.12 | 0.45 |
| 13:44 p.m | 32.16 | 36.69 | 22.34 | 935 | 0.129 | 0.40 |
| 13:59 p.m | 31.67 | 35.77 | 24.62 | 897 | 0.101 | 0.38 |
| 11:41 a.m | 39.08 | 43.38 | 23.24 | 940 | 0.191 | 0.38 |
| 11:56 a.m | 39.75 | 43.92 | 22.59 | 951 | 0.202 | 0.36 |
| 13:14 p.m | 40.22 | 43.82 | 20.26 | 915 | 0.237 | 0.32 |
| 13:29 p.m | 40.67 | 44.46 | 21.72 | 889 | 0.234 | 0.35 |
| 12:01 p.m | 49.15 | 52.82 | 22.42 | 878 | 0.325 | 0.34 |
| 12:16 p.m | 49.32 | 52.65 | 21.50 | 906 | 0.325 | 0.30 |
| 13:11 p.m | 49.89 | 52.52 | 22.01 | 918 | 0.318 | 0.23 |
| 13:26 p.m | 49.15 | 51.65 | 21.68 | 918 | 0.312 | 0.22 |

Source: Kaci et al (2012)

From Equation (1) and obtained measured values (Table 2), the characteristic curve of the instantaneous efficiency related to the inlet temperature can be plotted. This curve will satisfy the equation 2:

$$\eta = 0.49 - 5.7 T^* \tag{2}$$

The value 0.49 represents the optical efficiency of the collector η_0 . It is the intersection of the curve with the y-axis. The value 5.7 represents the overall thermal losses of the collector a_1 which is the slope of the line.

The incidence angle modifier is a correction factor for the effective transmissivity-absorptivity product $K_{\tau\alpha}$ is defined as the ratio of the instantaneous efficiency at any incidence to the efficiency at normal incidence. It allows you to calculate the instantaneous return at any incidence of the day (Kaci et al 2012).

$$K_{\tau\alpha} = \frac{\eta(\theta)}{\eta(\theta=0)} \tag{3}$$

With $(\tau\alpha)_\theta$: Optical efficiency of the collector at normal incidence; $(\tau\alpha)_n$: Optical efficiency of the collector at θ incidence.

The incidence angle modifier tests were carried out by measuring the previous parameters (Te, Ts, Ta, I_g) at different angle of incidence θ (°). Six points are recorded: Two readings in the morning at an incidence of $-40^\circ < \theta < -50^\circ$; Two readings around noon TSV ($\theta < 15^\circ$) and two in the afternoon ($40^\circ < \theta < 50^\circ$). Table 3 shows the experimental values for the of the modified angle of incidence of the solar collector studied. The adjustment of the measurement points of the modified angle of incidence $K_{\tau\alpha}$ as a function of the angle of incidence θ is presented in parabolic form, as shown in Figure 6.

Table 3
Experimental values noted for the calculation of $K_{\tau\alpha}$ (Kaci et al, 2012)

| Points | θ (°) | T*(Km ² /W) | η | $[(1/\cos\theta)-1]$ | $K_{\tau\alpha}$ |
|--------|--------------|------------------------|-------|----------------------|------------------|
| 01 | -55 | 0.028 | 0.391 | 0.6689 | 0.836 |
| 02 | -50 | 0.034 | 0.343 | 0.555 | 0.734 |
| 03 | 0 | 0.076 | 0.468 | 0 | 1 |
| 04 | 15 | 0.049 | 0.452 | 0.025 | 0.966 |
| 05 | 50 | 0.110 | 0.320 | 0.657 | 0.685 |
| 06 | 55 | 0.063 | 0.327 | 0.750 | 0.699 |

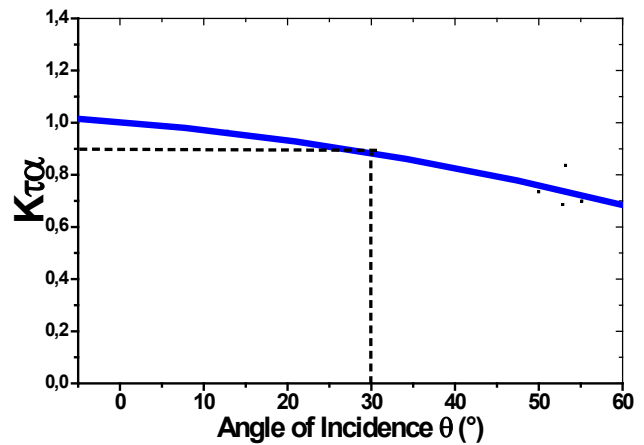


Fig. 6 Angle of incidence modified according to the angle of incidence θ

Table 4
Main parameters used in the simulation

| Parameter | Value | Unit |
|---|-------------------|---------------------|
| Weather data | Algiers (Algeria) | (-) |
| Collector aperture area | 2.6 | m ² |
| Collector type | Flat plate | (-) |
| Optical efficiency | 0.49 | (-) |
| Heat loss coefficients - a1 | 5.7 | W/m ² K |
| The incidence angle modifier $K_{\tau\alpha}$ | 0.87 | (-) |
| Collector loop-specific mass flow | 0.02 | kg/s m ² |
| Tilt angle | 36 | ° |
| Storage | 3000 | Liters |
| Process temperature | 60 | °C |

Source : Experimental tests (Kaci et al 2012); Laboref company report (2020)

The results of the evolution $K_{\tau\alpha}$ as a function of θ give a second-order curve in parabolic shape. It can be noticed that $K_{\tau\alpha}$ is more or less constant in the range of angle of incidence lower than 40° . With prismsed solar glass, the instantaneous efficiency of the flat solar collector can be constant up to an angle of incidence of 60° . It reaches a maximum for a value equal to 1. The values of $K_{\tau\alpha}$ are all less than one 1, which is true for the flat solar collector, because the latter reaches a maximum efficiency for a normal incidence the minimum value is 0.74, for this the average value is of 0.87 will be taken throughout our study. The latter represents a correction coefficient that must be multiplied by the expression of the performance of the capture field. Table 4 summarizes the technical characteristics of the experienced solar collector and a technical report obtained from the company (Laboref., 2020), (Laboref: Agro-food industry for the production of aromas).

2.4. System design

The objective this part is to determine the collector field area and its optimal configuration (series-parallel arrangements). The F-chart method, which is the most used method in the sizing of solar heating systems, is used to determine the solar collector field size. The F-chart method was developed by Klein and Beckman, using results obtained on a large number of simulations with TRNSYS. According to this model, the useful energy gained by a solar collector can be given by (Bangura et al 2022):

$$Q_u = A_c [F_R(\tau\alpha)_e I_g - F_R U_g (T_e - T_a)] \tag{4}$$

In our work, this model was improved by introducing the measured performance correction factor $K_{\tau\alpha}$ at any incidence for flat plate solar collectors. This correction is among the originalities of this work (Bangura *et al* 2022):

$$Q_u = A_c [K_{\tau\alpha} F_R (\tau\alpha)_e I_g - F_R U_g (T_e - T_a)] \quad (5)$$

Using the average values of collector's parameters obtained in the previous section ($K_{\tau\alpha} = 0.87$, $F_R (\tau\alpha)_e = 0.49$ and $F_R U_g = 6.53$), equation (5) become:

$$Q_u = A_c [0.87 \cdot 0.49 I_g - 6.53 (T_e - T_a)] \quad (6)$$

This method provides an useful mean for estimating the fraction of total heating load that will be supplied by solar energy for a given solar heating system. The primary design variable is collector area and secondary variables are collector type. Then, the solar fraction is defined by the equation 7 (Zwalnana *et al* 2021):

$$f = \frac{Q_u}{L} \text{ or } f = 1 - \frac{Aux}{L} \quad (7)$$

With L : Monthly total heating load for heating hot water; Aux : Monthly total heating auxiliary energy hot water; By replacing the expression of the useful energy in equation (7):

$$f = \frac{1}{L} \int_{\Delta t} A_c F_R [(\tau\alpha)_e I_g - U_g (T_e - T_a)] dt \quad (8)$$

Where :

$$Z = \frac{T_e - T_a}{T_{ref} - T_a}$$

Therefore, the equation (8) becomes:

$$f = \frac{A_c F_R}{L} \int_{\Delta t} [(\tau\alpha)_e I_g - U_g (T_{ref} - T_a) Z] dt \quad (9)$$

The method is a correlation of many hundreds simulation results of thermal solar system performances. The conditions of the simulations were varied over appropriate ranges of parameters for practical system designs. The resulting correlations give f , the fraction of monthly heating loads (hot water) supplied by solar energy as a function of two dimensionless parameters. The first is related to the ratio of collector losses and the second is related to the ratio of absorbed solar radiation.

This equation can be decomposed into 2 dimensionless terms X (Collector Loss) and Y (Collector Gain), which are given in equations (10) and (11) (Klein *et al* 2013 and Okafor *et al* 2012):

$$X = \frac{A_c F_R}{L} U_g (T_{ref} - \overline{T_a}) \Delta t \quad (10)$$

$$Y = \frac{A_c F_R}{L} (\tau\alpha) H_{\beta} N \quad (11)$$

For the system configuration studied, the solar fraction f of the monthly total load supplied by water heating system, given as a function of X and Y in equations 10 and 11, becomes in the form (Deepika *et al* 2016):

$$f = 1.029Y - 0.065X - 0.245Y^2 + 0.0018X^2 + 0.0215Y^3 \quad (12)$$

The iterative dichotomy method is used to solve equations (10), (11) and (12) which allow to obtain the collector's area for any incidence angle modifier.

Concerning the optimal configuration of solar system, the latter is designed according to the water temperature of the storage tank. The thermal collectors of the solar field may be connected in series, in parallel, or in combinations. Once the collector parameters, the storage size and loss coefficient, the magnitude of the load, and the meteorological data are specified, the storage tank temperature can be calculated as a function of time. Also, the energy gained from the collector, losses from storage, and energy to load can be determined for any desired period of time by integration of the appropriate rate quantities with the following equation (Kaci *et al* 2014).

$$(Mcp)_s \frac{dT_s}{dt} = A_c F_R [(K\tau\alpha)_e I_g - U_g (T_i - T_a)] - (UA)_s (T_s - T_a) - \varepsilon_2 (\dot{m}c_p)_{min} (T_s - T_r) \quad (13)$$

Equation (13) can be integrated using simple Euler method, where temperature derivative $\frac{dT_s}{dt}$ is expressed as $\frac{T_s^+ - T_s}{\Delta t}$. The time step should be taken equal to weather data increments in order to ensure numerical stability.

The storage temperature T_s can be given by (Kaci *et al* 2014):

$$T_s^+ = T_s + \frac{dt}{(mcp)_s} \{ \varepsilon A_c F_R [K(\tau\alpha) I_g - F_R U_g (T_e - T_a)] - (UA)_s (T_s - T_a) - \varepsilon (\dot{m}c_p)_s (T_e - T_r) \} \quad (14)$$

T_s^+ : The new tank temperature calculated for the end of the hour.

2.5. Economical parameters

The Levelized Cost of Energy (LCOE) is the most indicator to evaluate the competitiveness of the proposed solar thermal process. Indeed, LCOE represents the average revenue per unit of energy generated that would be required to recover the costs of operating the thermo-solar process during an assumed financial life cycle.

According to the International Energy Agency (IEA), The costs of the thermo-solar process can be classified into three different sets: investment costs, operation and maintenance costs and electricity costs. The factor multiplying the initial investment is called capital recovery factor (Crf). It converts a present value into a stream of equal annual payments over a specified time (in this case 25 years), at a specified discount rate (in this case 8%) (Fernández 2013).

$$LCOE = \frac{Crf \cdot K_{inv} + K_{O,M} + K_{electricity}}{E_{net}} \quad (15)$$

$$Crf = \frac{K_d(1+K_d)^n}{(1+K_d)^n - 1} + K_{insurance} \quad (16)$$

Where LCOE is the Levelized Cost of Energy, C_{rf} is the capital recovery factor, K_{inv} is the total investment of the plant, $K_{O\&M}$ is the annual operation and maintenance costs, $K_{electricity}$ is the annual electricity costs (7 DZD/kWh), E_{net} is the annual net thermal energy, K_d is the real debt interest rate = 8 %, n is the depreciation period in years = 25 years, $K_{insurance}$ is the annual insurance rate = 1 %.

3. Results and discussions

3.1. Solar field area and optimal configuration

In this section, the optimal solar collector area and system configuration using F-chart method are investigated. The thermo-solar system is sized based on the real parameters of the

collector measured in the experimental section. In Figure 7, it is shown the variation of the surface area of solar collector in function of the incidence angle and incidence angle modifier during a typical day of the year. Figure 7a shows that the collector area varies inversely proportional with the θ and $K_{\tau\alpha}$. That means that the closer the collector is to normal incidence ($K_{\tau\alpha} = 1$ or $\theta = 0$) the more the collector's efficiency increases which obviously induces a minimum surface. This result is in accordance with that found by Duffie *et al* (2013).

In our case, as shown in Figure 7a and Figure 7b, for $\theta = -30^\circ$ (East) and $\theta = +30^\circ$ (West) and where a value of incidence angle modifier of 0.87 is considered (Figure 6), an area of 64 m² is obtained, which corresponds to a number of 24 collectors (the collector used has a unit area of 2.6 m²). In order to determine the optimal configuration of the solar field, four cases are considered in function of the number of solar collectors in series. The cases consider two, three, four collectors in series and in the last case all collectors are connected in parallel. The variation of the storage tank temperature for the four different cases studied is shown in Figure 8.

It was observed that the higher the number of collectors in series, the higher the water outlet temperature. However, only the configuration with four collectors in series is able to reach the operating temperature of the industrial process (60°C) during the period of hot water utilization, as well Nunes *et al* (2014) reported in their work. Therefore, the solar system will be composed of 6 blocks of collectors in parallel with 4 collectors in series in each block, (i.e. 24 collectors).

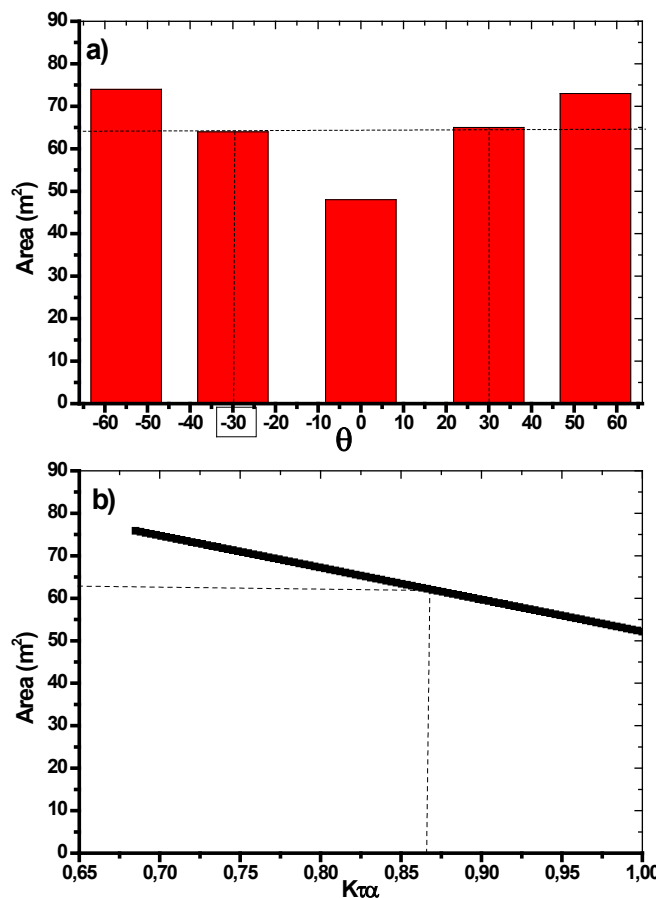


Fig. 7 Determination of the collector's areas: a) a function of Incidence Angle; b) a function of incidence Angle Modifier

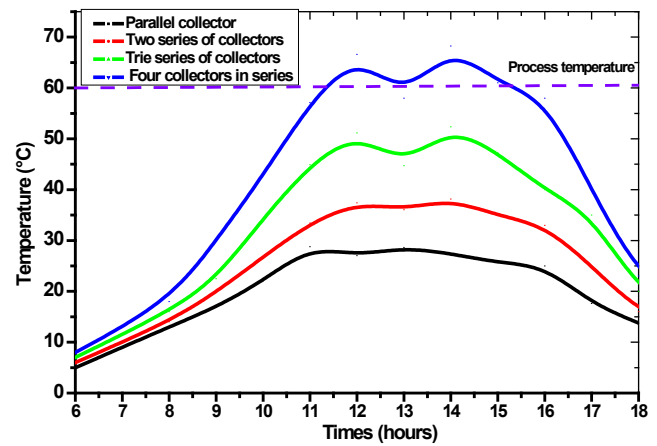


Fig. 8 storage tank Temperature during a day

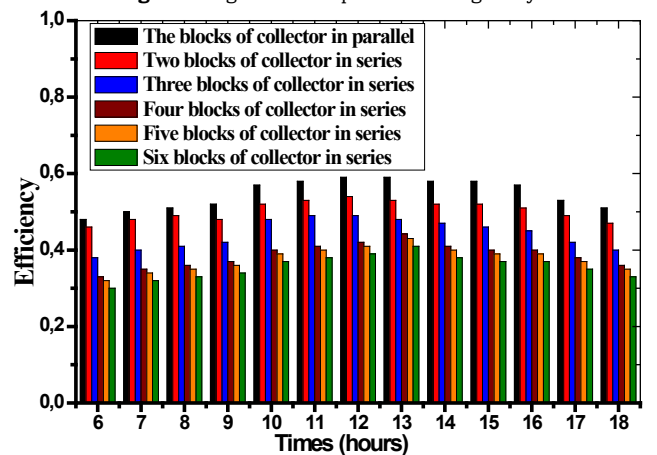


Fig.9 Variation of the collector's efficiency in function of the block's configurations

Effectively, the result shows that the efficiency of the configuration of 6 blocks in parallel is better than that of configurations with blocks in series, as shown in Figure 9. Indeed, the blocks of collectors connected in series induce greater heat losses by convection and radiation and therefore result in a lower thermal efficiency. This design is more efficient from an economic point of view because the comparison of different configurations also indicates that series configurations result in additional pressure drop, which also increases the pumping power (Duffie *et al.* 2013)

3.2. Solar fraction of the solar system

The energy performance the solar system under investigation is determined by calculating the solar fraction of the solar system. The solar fraction is defined as the ratio of the thermal energy produced by the solar collectors and the thermal energy needed for hot water production required by the industrial process (Ghafour, 2014). In this work, Eq.12 was used to calculate the hourly, monthly and yearly solar fraction

Considering the variations of the mains water temperature (shown in Fig.4) and rhythms of industrial production (hourly daily hot water need, Fig.2), the monthly energy needs of hot water production are represented on Figure 10. This figure illustrates also the global monthly solar radiation available in this location. We note that, unfortunately, the maximum needs

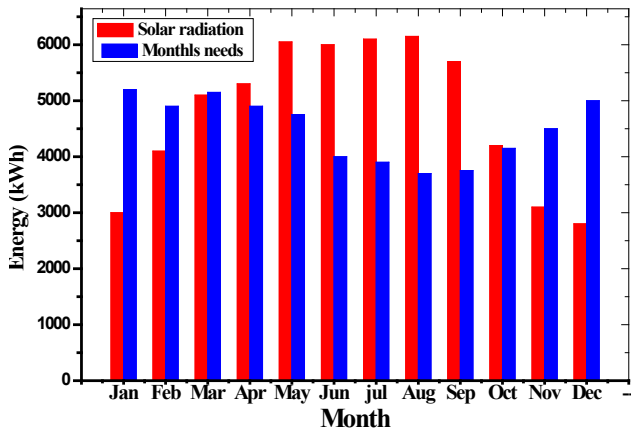


Fig.10 Monthly solar radiation and monthly energy needs

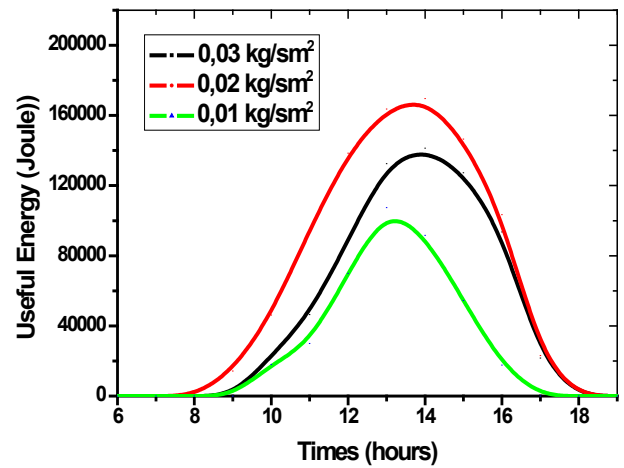


Fig. 12 Effect of mass flow rate on the useful energy gain

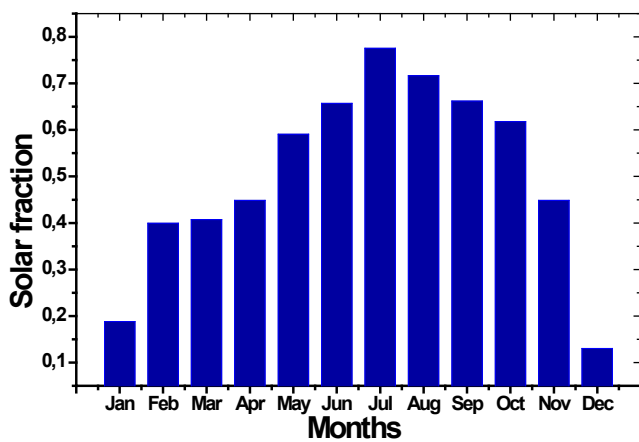


Fig. 11 Variation of solar Energy efficiency during a year

for hot water correspond to the periods when the availability of solar energy is minimal. Indeed, solar radiation energy is high in summer. It reaches up to (6000 kWh) while in winter it is about 2500 kWh. Solar energy could be enough to deliver the required amount of hot water during summer. During winter, the solar coverage rate is inevitably lower than in summer as shown in Figure 10. It is therefore necessary to properly size the installation to obtain the best energy/economic compromise.

Figure 11 represents the monthly solar fraction of the solar system. It can reach a maximum of 80% in summer, with an average annual solar fraction of about 50%. This is due to the best proposed design, the optimal operating parameters chosen for the system and the high intensity of solar radiation at the site. In the work conducted by Pahlavan *et al* (2018), where a water heating solar system is applied in 37 regions in Algeria, a yearly solar fraction of 60% was found, which is very close to our results. This means that such systems are very interesting.

3.3. Parametrical study

In order to determine the optimum flow rate for the optimum solar collector's configuration found in the previous section, water mass flow rate varying between 0.01 kg/m²s and 0.04 kg/m²s are considered, which are the most useful flow rate range for solar heating installations (Duffie *et al* 2013). The aim was to determine the optimum flow for this configuration of solar collectors. It was observed that this configuration offers the best solar fraction when the mass flow rate is 0.02 kg/s m².

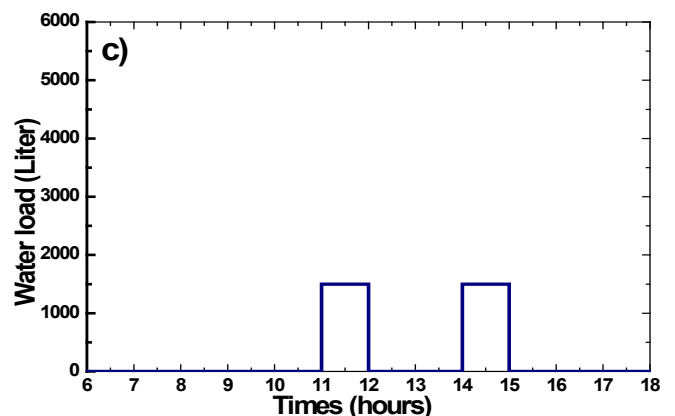
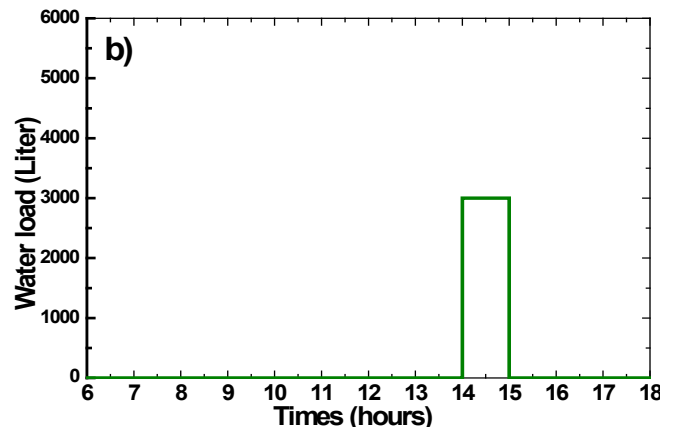
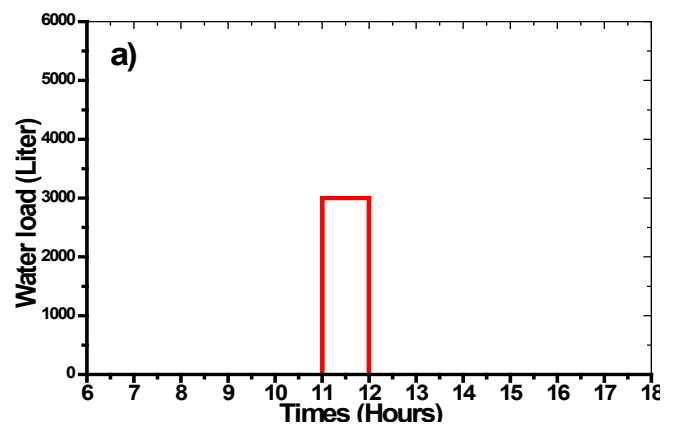


Fig. 13 Storage capacity for three different cases load profile a) in morning b) afternoon c) shared between hand and afternoon

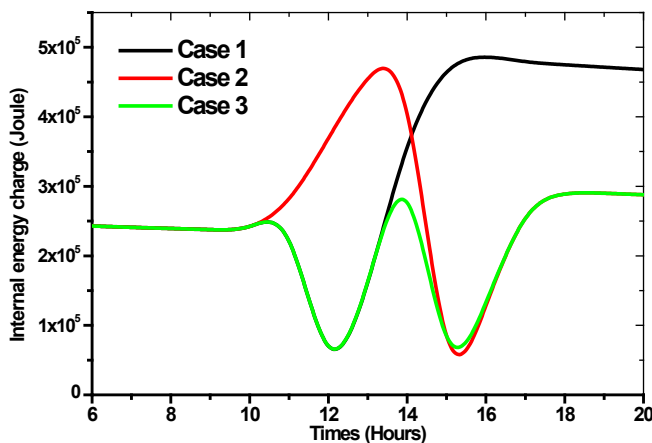


Fig. 14 Effect of the water load moment on the performance of the installation

This is the optimum value of mass flow rate for solar water heating systems recommended by ISO 9806 and EN 12975-2 (Kramer *et al.* 2017) and which is used throughout this work. The results find in this study are also in agreement with those of Hang *et al.* (2012) and Ge *et al.* (2012). As shown in Figure 12, for all cases considered the mass flow rate increase gradually with heat flux until reaching its maximum in the middle of the day and then decrease with the falling of the sun. The collector efficiency shows a proportional relationship with the mass flow rate (Mandal and Ghosh, 2020; Yassen *et al.*, 2019).

The influence of the load profile is investigated for different cases. A real load profile was used as an input for the model in the brewing water loop to consider the manual interference of the discharge control. It has been considered three cases to highlight the effect of water load on the effectiveness of the installation, as shown in Figure 13. The hot water demand occurs, in the first, second and third cases, respectively, in morning (Fig.13a), afternoon (Fig.13b), and shared between morning and afternoon (Fig.13c).

It can be seen from Figure 14, which represents the effect of the water load moment on the performance of the installation, that the efficiency of the case with a water load in the afternoon (case 2) is higher than that in the morning (case 1). Indeed, in the latter case, the storage tank is less charged with solar energy and the storage tank will be recharged with cold water, which induces significant heat losses. It has been observed that the water load in the morning or in the evening has a significant effect on the performance of the installation. Therefore, the best system performance is achieved when the water load is occurred in the afternoon.

It can also be observed from Figure 14, which shows the effect of the number of waters loads on the performance of the installation, that the efficiency of the case with one water load (case 1 and 2) is higher than that with two water loads (case 3), nearly double. This is because in the latter case the storage tank is re-charged with cold water, which also induces significant heat losses. It has been observed that the number of water load during the day has strongly effect of the performance of the installation. This means that processes that operate during many days in the week are not always preferable unless the total load is higher. It can be concluded that the load profile is expected to be the most important influence factors for the system performance of a solar process. Indeed, the work of Schmitt *et al* (2012) also shows that the load profile is the most important influencing factor for the system performance of a solar process heat system;

4. Economical study

After the design phase, the system is investigated in economical point of view. For this reason, various costs of the project components are estimated. Table 5 illustrates the costs of each component of the thermo-solar process.

As illustrated in Table 6, three cases have been considered:

Case 1: Solar system without support (subvention) from the Algerian government program of renewable energy;

Case 2: Solar system with support. The Algerian government program of renewable energy offers 45% of the total costs of solar collectors (APRUE 2022).

Case 3: Conventional system. The heating system is powered by the electrical energy from the grid.

The net annual energy produced is calculated taking into account the technical report from the company, that is to say process temperature of 60 °C and the average daily hot water of 3000 liters. The solar processes (Cases 1 and 2) are supposed to ensure 50 % of the energy needs (result found in Figure 6 average annual solar fraction of about 50 %), which results in annual electricity demand of 25 080 kWh. Table 6 shows the actual LCOE in the Algerian market for an electricity price of 7DZD/kWh, which is equivalent to 0.05 €/kWh.

Table 5

Costs of each part of the industrial process

| Component | Unit cost (€) | Number | Total cost (€) |
|---------------------------------|---------------|--------|----------------|
| Investment costs | | | |
| Collectors | 505.52 | 24 | 12 132.48 |
| Piping | 25.28 | 200 | 5 056 |
| Gate valve | 27.33 | 30 | 819.9 |
| Safety valve | 13.66 | 12 | 163.92 |
| Monometer | 21.86 | 5 | 109.3 |
| Purge | 10.25 | 30 | 307.5 |
| Check valve | 13.66 | 10 | 136.6 |
| Tank | 1024.7 | 2 | 2049.4 |
| Pumps | 314.57 | 5 | 1572.85 |
| Vase expansion | 51.23 | 1 | 51.23 |
| Heat Exchanger | 512.35 | 2 | 1024.7 |
| Temperature Regulator | 81.98 | 2 | 163.96 |
| Operation and maintenance costs | | | |
| Collectors | 6.83 | 24 | 163.92 |
| Tanks | 153.7 | 2 | 307.4 |
| Piping | 170.78 | 1 | 170.78 |

Source : Missoum *et al* (2021)

Table 6

Total costs of the water heating processes

| Case | Kinvest (€) | KO&M (€) | Enet (kWh) | Electricity needs (KWh) | LCOE (DZD/kWh) | LCOE (Euro/kWh) |
|--------|-------------|----------|------------|-------------------------|----------------|-----------------|
| Case 1 | 23587.84 | 742.1 | 50160 | 25080 | 12.650 | 0.108 |
| Case 2 | 12973.31 | 742.1 | 50160 | 25080 | 9.071 | 0.067 |
| Case 3 | 3415.67 | 3204.94 | 50160 | 50160 | 8.246 | 0.061 |

1DZD = 0.0069 € (Source : External Bank of Algeria., 2023)

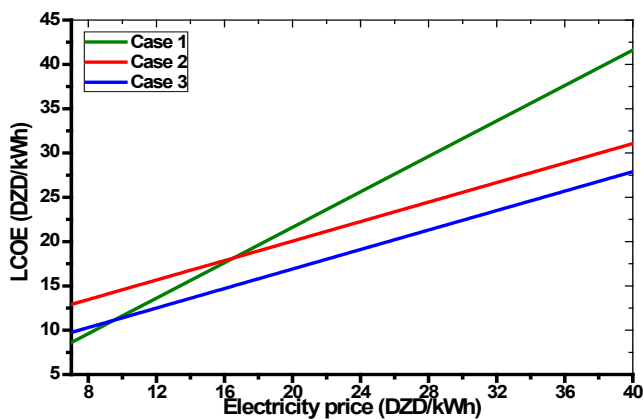


Fig. 15 Variation of LCOE as a function of electricity price.

The latter value is so much lower than international markets. For instance, the electricity price in Germany is about six times more expensive than in Algeria (0.30 €/kWh). Under the current scenario, the LCOE of the solar thermal process is 0.1€/kWh, but its price with support is 0.067 €/kWh, slightly higher than the one based on electric heating (fossil fuels-based processes) is 0.061€/kWh, a very encouraging result.

Figure 15 shows the variation of the LCOE of the three processes (Cases 1, 2, 3) as a function of electricity prices. A range from 0.048€ to 0.27€/kWh is intentionally considered. The former value is the actual price in the Algerian market while the latter is the price in the German market. As showing in Figure 15, the solar process with support is becoming competitive to the fossil-based heating process at the electricity price of 0.061€/kWh; a price corresponds to US and Canada markets. For the case of a solar process without support from the Government, the electricity price should rise to about 0.12€/kWh to ensure competitiveness. This price corresponds to the French electricity market.

5. Comparison of results

To verify and justify the results we obtained, they were analyzed and compared with the results of two different process heating systems, as shown in Table 7, with the same collector technology (flat plate collector), flow rate and set-point water heating temperature T_c (60 °C). Therefore, the solar fractions of the obtained systems are relatively similar. To verify and justify the obtained results, they were analyzed and compared with the results of two different process heating systems, as shown in Table 7, with the same collector technology (flat plate collector), flow rate and set-point water heating temperature T_c (60 °C). Therefore, the solar fractions of the obtained systems are relatively similar.

Bahria *et al.*, (2016) investigated the performance of a solar heating system in different climates of Algeria. The solar fraction for domestic hot water of 80% has been found. Kalogirous *et al.*(2003) studied a solar industrial process heat in Chypre. The solar fraction of system was 75%. In other work, the authors Kalogirous *et al.*(2019), have found for the same system, a LCOE of 0.2 Euro/kwh. Moreover, for the work presented by Sturm *et al.* (2015) on the case study of a medium sized Beijing based factory, the result also gave the fraction of 14% and the LCOE of 0.14, which also confirms the accuracy of our result. However, the resulting energy costs (LCOE) obtained for solar heat are 0.1 €/kWh. These results are applicable to all countries with similar weather and economic conditions to these regions. The small difference in the LCOE lies mainly in the price of conventional energy in Algeria is subsidized which makes its price a bit low compared to other cases

Table 7

Comparison of results to others studies

| Case | Solar potential (kWh/m ²) | Collector: type | Flow rate (Kg/sm ²) | T _c (°C) | Solar fraction | LCOE (€/kWh) |
|----------------------------|---------------------------------------|-----------------|---------------------------------|---------------------|----------------|--------------|
| This study | 1651 | (FPC) | 0.02 | 60 | 50 % | 0.1 |
| Bahria <i>et al</i> 2016 | 1800 | (FPC) | 0.02 | 60 | 82% | - |
| Kalogirou 2003, 2019) | 1727 | (FPC) | 0.015 | 60 | 75% | 0.2 |
| Sturm <i>et al.</i> (2015) | 1400 | (FPC) | 0.02 | 60 | 14% | 0.1 |

6. Conclusion

This study presents the results of the design, size and energy efficiency of a solar thermal system for the food industry in Algeria. The method used to size the system is based on the F-chart method of the HWB model, improved by introducing a new power correction factor at each flat-plate incidence angle, which was one of the original features of this work. This value has been experimentally tested and calculated according to the EN 12975-2 standard, using real data of energy demand and water consumption curves to determine the actual solar process performance. The results obtained after simulating the model used resulted in a collection arrangement taking into account the requirements, process temperature and the available area of 64 m² (i.e. 24 collectors) on the company's roof.

The system consists of 6 collector blocks connected in parallel, with 4 collectors connected in series in each block. Simulation results show that a solar coverage of 50% per year can be achieved, which is very high and has sparked great interest in integrating this solar thermal process at selected locations.

The parametric study confirmed that the selected mass flow rate is in good agreement with the EN 12975-2 and ISO 9806 standards. The results also showed that the amount and duration of water exposure during the day had a large impact on plant performance. Therefore, to keep up with the fluctuations of the sun, the best time to brew is in the afternoon or early evening.

The sensitivity analysis shows that operating temperature, collector selection, and required power are the most important factors affecting system efficiency. The economic evaluation shows that the assisted solar process is competitive with the fossil heating process at an electricity price of 0.062€/kWh, while the unassisted solar process may be more competitive when the electricity price reaches 0.12€/kWh. In the current context of global warming, Algeria's energy transition is still hampered by the relatively high installation costs of renewable energy compared to the kWh price of fossil electricity. The same is true for most oil and gas production operations. In fact, the latter's current offer is unbeatable. Therefore, it is more urgent than ever to develop national economic development plans that promote energy and environmental transition and sustainable development.

Nomenclature

| | |
|----------|--|
| A_{c1} | Collectors' area of the first collector (m ²) |
| A_{c2} | Collectors' area of the second collector (m ²) |
| A_c | Collectors' area (m ²) |
| C_p | Heat capacity of water (kJ/kg°C) |
| F | Fraction of the monthly heating load(-) |
| F' | Corrected F_R factor (-) |
| F_R | Collector heat exchanger efficiency factor (-) |

| | |
|-------------|--|
| F'_R | Corrected collector heat exchanger efficiency factor (-) |
| F_{RU_g} | Collector overall energy loss coefficient ($W/m^2\text{ }^\circ\text{C}$) |
| Gh | Monthly averaged, daily radiation incident (MJ/m^2) |
| H_{β} | Monthly average daily radiation incident on collector surface per unit area (MJ/m^2) |
| h_m | Sun height (degree) |
| I_g | Global solar radiation (W/m^2) |
| L | Monthly total heating load hot water (kWh/m^2) |
| M | Actual mass of storage capacity (kg) |
| \dot{m} | Mass flow rate (kg/s) |
| N | Days in month(-) |
| Q_{u1} | Solar useful heat gain rate of the first collector(W) |
| Q_{u2} | Solar useful heat gain rate of the second collector (W) |
| T_e | Inlet fluid temperature ($^\circ\text{C}$) |
| T_a | Ambient temperature ($^\circ\text{C}$) |
| T_{ref} | An empirically derived reference temperature ($^\circ\text{C}$) |
| T_r | The mains water temperature ($^\circ\text{C}$) |
| TS | Storage temperature ($^\circ\text{C}$) |
| \bar{T}_a | Monthly average ambient temperature ($^\circ\text{C}$) |
| T_d | The minimum desired temperature($^\circ\text{C}$) |
| X | Modified sensibility factor of the thermal losses (-) |
| \bar{X}_C | Dimensionless average daily critical level of the solar collector (-) |
| Y | Ratio of the absorbed solar energy to the cooling load (-) |

Greek symbols

| | |
|------------------|---|
| Δt | Total number of seconds in month (s) |
| β | Collector tilt angle (degree) |
| ε | Heat exchanger effectiveness (-) |
| $(\tau\alpha)_e$ | Monthly average transmittance-absorptance product (-) |

Abbreviations

| | |
|-----|------------------------------|
| IAM | Incidence Angle Modifier (-) |
| TSV | True solar time (hours) |

References

- APRUE. The National Agency for the Promotion and Rationalization of Energy Use, (2022) Development of the regulatory and incentive framework for energy efficiency in Algeria), *ALSOL-Programm*. <https://www.aprue.org.dz>
- Mounir, A., Rima, Z., Aziz, N. (2013). Technical-Economic Analysis of Solar Water Heating Systems at Batna in Algeria. In: Hakansson, A., Höjer, M., Howlett, R., Jain, L. (eds) Sustainability in Energy and Buildings. Smart Innovation, Systems and Technologies, vol 22. Springer, Berlin, Heidelberg. https://doi.org/10.1007/978-3-642-36645-1_70
- Anubhav, U., Kesari, J. P., Zunai. M., (2016) Designing of Solar Process Heating System for Indian Automobile Industry. *International journal of renewable energy research*, 6(4). 1627-1636. <https://doi.org/10.20508/ijrer.v6i4.4490.g6956>
- Bahria, S., Amirat, M., Hamidat, A, El Ganaoui, M, Slimani, M. A. (2016). Parametric study of solar heating and cooling systems in different climates of Algeria—A comparison between conventional and high-energy-performance buildings. *Energy*, 113, 521-535 <https://doi.org/10.1016/j.energy.2016.07.022>
- Bangura, A. B. M., Hantoro, R., Fudholi. A. (2022) Mathematical Model of the Thermal Performance of Double-Pass Solar Collector for Solar Energy Application in Sierra Leone. *International Journal of Renewable Energy Development*, 11(2), 347-355. <https://doi.org/10.14710/ijred.2022.41349>
- Center for the development of renewable energies in Algeria., (2021) Radiometric station. <https://www.cder.dz/?lang=en>
- Deepika, D., Baig, M. A., Reddy, A. R., Maneaih, D. (2016). Utilization of f-Chart Method for Designing Solar Thermal Heating System. *Journal of Mechanical and Civil Engineering*, 5, 23-28, <https://doi.org/10.9790/1684-16053042328>
- Desai, D.D., Raol, J.B, Patel, S, Chauhan, I. (2013) Application of solar energy for sustainable dairy development. *Eur J Sustain. Dev.* 2, 131-40. <https://doi.org/10.14207/ejsd.2013.v2n2p131>
- Duffie, J. A., William, A., Beckman, A. W. (2013) Solar Engineering of Thermal Processes. 4th Ed. Published by John Wiley & Sons; <https://doi.org/10.1002/9781118671603>
- Farjana, S. H., Huda, N., Parvez., Mahmud, M.A. and Saidur. R. (2017) Solar process heat in industrial systems – A global review. *Renewable and Sustainable Energy Reviews*. 82(3), 2270-2286, <https://doi.org/10.1016/j.rser.2017.08.065>
- Fernández, A. C. (2013) Economic Study of Solar Thermal Plant based on Gas Turbines. *Master Thesis; LTH School of Engineering*. <http://hdl.handle.net/2099.1/19690>
- Fuller, R.J., (2011) Solar industrial process heating in Australia, Past and current status. *Renewable Energy*, 36, 216-221; <https://doi.org/10.1016/j.renene.2010.06.023>
- Ge, T.S., Dai, Y.J., Li, Y., Wang, R.Z. (2012) Simulation investigation on solar powered desiccant coated heat exchanger cooling system. *Applied Energy*, 93, 532-540; <https://doi.org/10.1016/j.apenergy.2011.11.089>
- Ghafoor, A., Munir, A. (2014) Thermo-Economic Optimization of Solar Assisted Heating and Cooling (SAHC) System, *International Journal of Renewable Energy Development*, 3(3), 217-227. <https://doi.org/10.14710/ijred.3.3.217-227>
- Hang, Y., Qu, M., Zhao, F. (2012) Economic and environmental life cycle analysis of solar hot water systems in the United States. *Energy and Buildings*, 45, 181-188; <https://doi.org/10.1016/j.enbuild.2011.10.057>
- Intergovernmental panel on climate change IPCC (2022) mitigation of climate change; assessment report on climate change. <https://www.ipcc.ch/report/>
- James & James., (2010) Planning & Installing, Solar Thermal Systems. Fully revised & updated 2nd edition. London: Earthscan <https://doi.org/10.4324/9781849775120>
- Kaci, K., Laoudj, O., Merzouk, M., Kasbadji, N., Sami, H. (2014) Optimization of collector area for solar heating. *J. Macro Trends Health Med*. https://macrojournals.com/yahoo_site_admin/assets/docs/8E_S21al.960840.pdf
- Kaci, K., Merzouk, M., Kasbadji, N. (2012) Effect of Tests Norms on the Instantaneous Efficiency of a Plate Solar Collector. *Procedia Engineering* 33, 392-403; <https://doi.org/10.1016/j.proeng.2012.01.121>
- Kalogirou, S. (2003).The potential of solar industrial process heat applications. *Appl. Energy*. 76(4), 337–361; [https://doi.org/10.1016/S0306-2619\(02\)00176-9](https://doi.org/10.1016/S0306-2619(02)00176-9)
- Kalogirou, S. (2019) Applications of Renewable Energy Systems in Buildings and Industry; *Report of Department of Mechanical Engineering and Materials Sciences and Engineering*. <http://www.oeb.org.cy/wp-content/uploads/2019/11/3>
- Klein, K. A., Beckman, W. A., Duffie, J. A. (2013) A design procedure for solar heating systems. *Solar energy*. 18, 113-127. [https://doi.org/10.1016/0038-092X\(76\)90044-X](https://doi.org/10.1016/0038-092X(76)90044-X)
- Kramer, K., Mehnert, S., (2017) Guide to standard ISO 9806:2017 a resource for manufacturers, testing laboratories, certification bodies and regulatory, *Technical report*, <https://doi.org/10.13140/rg.2.2.30241.30562>
- Kummert, M., Andre, P., Nicolas, J. (2001). Optimal heating control in a passive solar commercial building. *Solar Energy*, 69, 103-116. [https://doi.org/10.1016/S0038-092X\(01\)00038-X](https://doi.org/10.1016/S0038-092X(01)00038-X)
- Laboref, SARL., Food and Beverage Company(2013), The technical report from the company.Laboref . <https://www.laboref-dz.com>
- Lima, T., Charamba, C.J. (2015) Solar water heating for a hospital laundry: A case study, *Solar energy*. 122, 737-748, <https://doi.org/10.1016/j.solener.2015.10.006>
- Mandal, S., Ghosh, S.K. (2020) Experimental investigation of the performance of a double pass solar water heater withreflector. *Renewable Energy*, 149, 631-640; <https://doi.org/10.1016/j.renene.2019.11.160>
- Meyers, S., Schmitt, B., Vajen, K. (2018) The future of low carbon industrial process heat: A comparison between solar thermal and heat pumps. *Solar Energy*. 173, 893-904. <https://doi.org/10.1016/j.solener.2018.08.011>
- Meteonorm 8. (2022). Meteonorm Software Worldwide Europe irradiation data. Intersolar Europe. <https://meteonorm.com/en/news>
- Ministry of Water Resources and Water Security, Algerian Waters , (2021), *Annual report*. <https://www.aps.dz/en>

- Missoum, M., Loukarfi, L. (2021) Investigation of a Solar Poly generation System for a Multi-Storey Residential Building-Dynamic Simulation and Performance Analysis. *Int. Journal of Renewable Energy Development*, 10(3), 445-458; <https://doi.org/10.14710/ijred.2021.34423>
- Müller, T., Weiß, W., Schnitzer, H., Brunner, C. (2004) Potential study on the use of thermal solar energy in Austrian commercial and industrial companies. *Annual Report*. <https://doi.org/10.1016/j.rser.2012.04.032>
- National Renewable Energy Laboratory. (2021) Decarbonizing industrial process heat, *annual report*. <https://www.frontiersin.org/journals/energy-research>
- Núñez, M. P., Odríguez, G. M., Amanda, L., Silva, F. (2014) Design of solar collector networks for industrial applications. *Applied Thermal Engineering*, 1-8. <https://doi.org/10.1016/j.applthermaleng.2014.05.005>
- Okafor, I. F., Akubue, G. (2012) F-Chart Method for Designing Solar Thermal Water Heating Systems. *International Journal of Scientific & Engineering Research*, 3-9, <https://citeseerx.ist.psu.edu/document?repid=rep1&type=pdf&doi=094d081464742e2226f7700239fcb6dc953cd0c5>
- Pahlavana, S., Jahangirib, M., Shamsabadic, A., Khechekhouche, A., (2018). Feasibility study of solar water heaters in Algeria, a review. *Journal of Solar Energy Research*, 3(2), 135-146. https://jsr.ut.ac.ir/article_67424.html
- Palaniappan, C., (2009). Perspectives of solar food processing in India:1–11. International Solar Food Processing Conference. https://solarcooking.fandom.com/wiki/International_Solar_Food_Processing_Conference_2009
- Quijiera, J.A., Alriols, M.G., Labidi, J. (2011). Usage of solar energy in an industrial process. *Chem Eng Trans*; 25, 875–80. <https://doi.org/10.3303/CET1125146>
- Renewable Energy Policy Network for the 21st Century. (2016) Global Status Report. *Annual Report*. <https://renewablepower.theiet.org>
- Schmitt, B., Lauterbach, C., Dittmar, M., Vajen, K., (2012). Guideline for the utilization of solar heat in breweries. *Proceedings Eurosun Rijeka, Croatia*.
- Schweiger, H., Farinha, M., Schwenk, C., Hennecke, K., (2000)The Potential of Solar Heat for Industrial Processes, Barcelona, Lissabon, München, Köln, Madrid, Spain, POSHIP. *Final report*. http://www.solarpaces.org/Library/docs/POSHIP_Final_Report.pdf
- Sharma, A., K, Sharma, C., Mullicka. S. C and Kandpala, T. C. (2017) Solar industrial process heating: A review. *Renewable and Sustainable Energy Reviews*, 78, 124–137. <https://doi.org/10.1016/j.rser.2017.04.079>
- Sturm, B., Meyers, S., Zhang, Y., Law, R., Eric, J., Valencia, S., Bao, H., Wang, Y., Chen, H. (2015) Process intensification and integration of solar heat generation in the Chinese condiment sector – A case study of a medium sized Beijing based factory. *Energy Conversion and Management*, 106, 1295-1308; <https://doi.org/10.1016/j.enconman.2015.10.045>
- Suresh, N.S. (2017) Solar Energy for Process Heating: a Case Study of Select Indian Industries. *Journal of Cleaner Production*, (151), 439-451. <https://doi.org/10.1016/j.jclepro.2017.02.190>
- The International Energy Agency. (2015) Process Heat Collectors: State of the Art and Available Medium Temperature Collectors, TASK 49. *Annual Report*. https://task49.iea-shc.org/Data/Sites/1/publications/Task%2049%20Deliverable%20A1.3_20160504.pdf
- The International Renewable Energy Agency. (2015) Solar Heat for Industrial Processes, Technology Brief E21. *Annual Report*. https://www.irena.org/-/media/Files/IRENA/Agency/Publication/2015/IRENA_ETSA_P_Tech_Brief_E21_Solar_Heat_Industrial_2015.pdf
- The International Renewable Energy Agency. (2015) Quality Infrastructure for Renewable Energy Technologies Solar Water Heater, *Annual Report*, <https://www.irena.org/publications/2015/Dec/Quality-Infrastructure-for-Renewable-Energy-Technologies-Solar-Water-Heaters>
- The International Renewable Energy Agency. (2015) Renewable Energy Options for the Industry Sector, Global and Regional Potential until 2030. *Annual Report*, https://www.irena.org/-/media/Files/IRENA/Agency/Publication/2014/Aug/IRENA_RE_Potential_for_Industry_BP_2015.pdf
- The International Energy Agency (IEA). (2020) Renewables 2019 analysis and forecast to 2024. *Annual report*; https://iea.blob.core.windows.net/assets/a846e5cf-ca7d-4a1f-a81b-ba1499f2cc07/Renewables_2019.pdf
- The Minister of Energy Transition and Renewable Energies., (2022). The Energies and Energy Efficiency Program. *Annual Report*; <https://www.energy.gov.cz>
- Valderrama, C., Cortina, J. L., Aliakbar, A., Bawahab, M. (2022) Solar ponds. *Storing Energy* (Second Edition), 2 537-558; <https://doi.org/10.1016/B978-0-12-824510-1.00004-0>
- Weiss, W., (2005) Solar heating worldwide, markets and contribution to the Energy supply, IEA, solar heating and cooling program. *Annual Report*. <https://www.iea-shc.org/Data/Sites/1/publications/Solar-Heat-Worldwide-2022.pdf>
- Zühlsdorf, B., Bühlere, F., Bantlec, M., Elmegaarda, B. (2019) Analysis of technologies and potentials for heat pump-based process heat supply above 150 °C. *Energy Conversion and Management X*, 2. <https://doi.org/10.1016/j.ecmx.2019.100011>
- Zwalnana, S. J., Duvunab, G. A., Abakra, Y. A., Badaa, T., (2021) Design and Performance Evaluation of a Multi-Temperature Flat Plate Solar Collector. *Int. Journal of Renewable Energy Development*, 10(3),537-549. <https://doi.org/10.14710/ijred.2021.33213>



© 2023. The Author(s). This article is an open access article distributed under the terms and conditions of the Creative Commons Attribution-ShareAlike 4.0 (CC BY-SA) International License (<http://creativecommons.org/licenses/by-sa/4.0/>)